

## Superconductivity in Iron Telluride Thin Films under Tensile Stress

Y. Han,<sup>1</sup> W. Y. Li,<sup>1</sup> L. X. Cao,<sup>1,\*</sup> X. Y. Wang,<sup>2</sup> B. Xu,<sup>1</sup> B. R. Zhao,<sup>1</sup> Y. Q. Guo,<sup>3</sup> and J. L. Yang<sup>2</sup>

<sup>1</sup>National Laboratory for Superconductivity, Institute of Physics and Beijing National Laboratory for Condensed Matter Physics, Chinese Academy of Sciences, Beijing 100190, China

<sup>2</sup>Institute of Semiconductors, Chinese Academy of Sciences, Beijing 100083, China

<sup>3</sup>School of Energy and Power Engineering, North China Electric Power University, Beijing 102206, China

(Received 11 November 2009; published 8 January 2010)

By realizing in thin films a tensile stress state, superconductivity of 13 K was introduced into FeTe, a nonsuperconducting parent compound of the iron pnictides and chalcogenides, with a transition temperature higher than that of its superconducting isostructural counterpart FeSe. For these tensile stressed films, superconductivity is accompanied by a softening of the first-order magnetic and structural phase transition, and also, the in-plane extension and out-of-plane contraction are universal in all FeTe films independent of the sign of the lattice mismatch, either positive or negative. Moreover, the correlations were found to exist between the transition temperatures and the tetrahedra bond angles in these thin films.

DOI: 10.1103/PhysRevLett.104.017003

PACS numbers: 74.70.-b, 68.03.Cd, 74.62.Fj, 74.78.-w

There is considerable interest in promoting transition temperature ( $T_c$ ) [1] and even introducing superconductivity by realizing in thin films a high-pressure state, i.e., an effect of the stress tensor. Stress in thin film is, for specified directions, the force per unit length of the substrate exerted across the interface on the elastically deformed film. Although an in-plane extension of the film is not forbidden in nature, the stress effect is generally believed to be an in-plane contraction analogous to the application of hydrostatic pressure on bulk materials [1]. Consequently, tensile stress in films is usually believed to be irrelevant for such a purpose and therefore is rarely studied.

Very recently, the discovery of superconductivity in iron pnictides [2] and chalcogenides [3] has triggered tremendous efforts to search for new superconductor materials and to raise their  $T_c$  by chemical doping [4–7] or by external pressure [8–11]. A corrugated layer comprising Fe and pnictogens (Pn = P, As) or chalcogens (Ch = Se, Te) incorporates with different interlayers leading to four structural families, among which binary iron chalcogenide FeSe and FeTe as well as their solid solution  $\text{FeSe}_{1-x}\text{Te}_x$  possess the simplest crystal structure with only the FeCh layers stacking one by another. In comparison with chemical doping which usually changes physical parameters in many different ways, hydrostatic pressure experiment can provide systematic study on salient physics, and therefore it is widely applied to study phase transitions and to raise  $T_c$  of the iron pnictides [8,9] and chalcogenides [10,11], including making parent compounds superconducting [9].

We report the superconductivity at 13 K in FeTe which is in the form of thin films and under the tensile stress, although bulk crystals are not superconducting at ambient pressure [12–14] or under high pressure [15,16]. The intriguing fact is, superconductivity appears when the first-order magnetic and structural phase transition softens, and when the Fe-Te-Fe bond angles become larger. Our demonstration of superconductivity introduced by extension of

lattice realized via interfacial stress paves the way for higher transition temperatures in iron chalcogenides by fine tuning the crystal structure through chemical doping and for better understanding of superconductivity mechanisms in this category of materials.

Over 100 FeTe films were pulsed laser deposited with chamber base pressure of  $4 \times 10^{-5}$  Pa and at  $\sim 540^\circ\text{C}$  under environment better than  $2 \times 10^{-4}$  Pa on (001)-oriented  $4 \times 5 \times 0.5 \text{ mm}^3$   $(\text{LaAlO}_3)_{0.3}(\text{SrAl}_{0.5}\text{Ta}_{0.5}\text{O}_3)_{0.7}$  (LSAT), MgO, SrTiO<sub>3</sub>, and LaAlO<sub>3</sub> substrates, respectively [17]. All films are superconducting. An XeCl excimer laser with a repetition rate of 4 Hz and power density of  $100 \text{ mJ mm}^{-2}$  was used, giving a deposition rate of 0.05 nm per laser pulse. Targets with nominal composition of  $\text{FeTe}_{1+x}$  ( $x = 0, 0.2, 0.4$ ) were vacuum sintered twice at  $\sim 600^\circ\text{C}$  for 24 h [17] with excess Te up to 40% to compensate volatile Te losses in FeTe films.

Although FeTe films deposited from a FeTe target without excess Te content are superconducting, epitaxial, and single phased as revealed by x-ray diffraction (XRD), some Fe-rich precipitates of  $\sim 500 \text{ nm}$  in size are found on surfaces of such films, 24 in total. Scanning electron microscopy (SEM) and energy dispersive analysis of x-ray (EDAX) give a Fe:Te ratio of  $\sim 8.9:1$  with electron beam focused on the precipitates.

All films given in this Letter, 86 in total, are deposited from the targets with nominal composition of  $\text{FeTe}_{1.4}$ . As shown in Figs. 1(a)–1(d), they are single-phased and (001) oriented. The  $c$ -axes lattice constants of the FeTe films were calibrated by those of substrate single crystals, as given in Fig. 1(e) for 32 films with thicknesses of 60, 90, 120, and 150 nm deposited on 4 different substrates at temperatures ranging from  $500^\circ\text{C}$  to  $580^\circ\text{C}$ . Thickness dependencies of the zero resistance transition temperature  $T_{c,0}$  reveal the maxima in 90 nm films, which suggest the critical thicknesses for pseudomorphic growth of these in-plane stretched films are  $\sim 90 \text{ nm}$  [18]. High-resolution

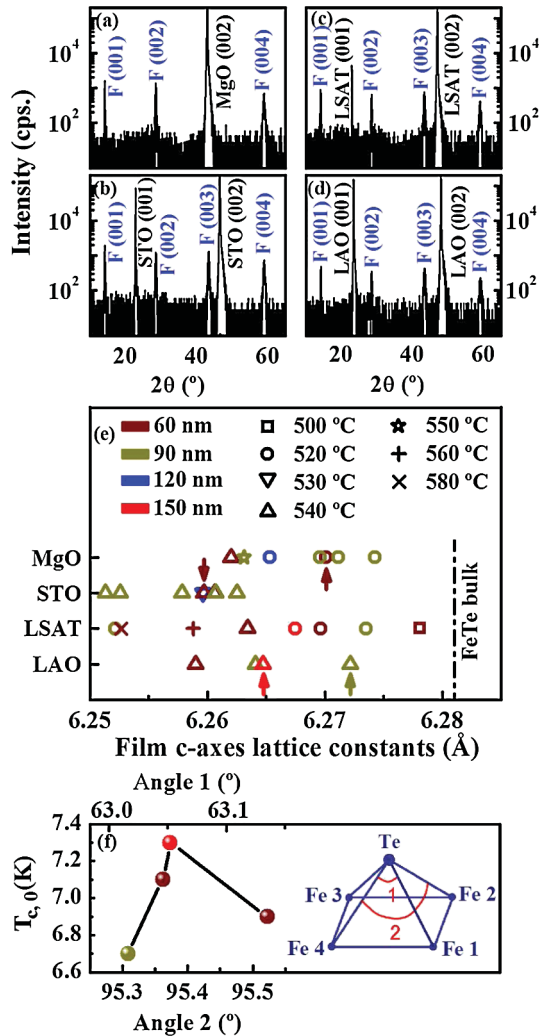


FIG. 1 (color). X-ray diffraction spectra measured at room temperature and related analysis. (a)–(d) XRD spectra of films on MgO, SrTiO<sub>3</sub>, LSAT, and LaAlO<sub>3</sub>, respectively, with *F* denoting film. (e) Summary of *c*-axes lattice constants for 32 FeTe films on 4 different substrates. Arrows indicate 4 samples the high-resolution XRD of which were performed to deduce the Fe-Te-Fe angles. (f) Fe-Te-Fe bond angle dependencies of zero resistance transition temperatures  $T_{c,0}$  for 4 FeTe films indicated by arrows in (e). Inset shows schematically the definition of the angle 1 and angle 2, which are Fe4-Te-Fe1 and Fe4-Te-Fe2, respectively.

XRD was performed on 4 out of 32 samples shown in Fig. 1(e) to obtain their *a* axis lattice constants, from which the Fe-Te-Fe bond angles can be estimated given in Fig. 1(f). Meanwhile, the Rietveld refinement was performed on a FeTe powder sample at 300 K. Minor amount of FeTe<sub>2</sub> (~7%) was found to coexist with Fe<sub>1.08</sub>Te phase, the *a*, *c*, Te *z* coordination, angle 1, and angle 2 of which are 0.38214(3) nm, 0.62875(3) nm, 0.2803(2), 62.64°, and 94.63°, respectively. This refinement result is in consistent with that given in Ref. [15].

One striking character is that the superconducting FeTe films change dramatically in the Fe-Te-Fe angles compared

to the nonsuperconducting Fe<sub>1+δ</sub>Te bulk samples. The increments of the angle 1 and angle 2 are ~0.4° and ~0.75°, respectively [Fig. 1(f)]. The bond angles dependencies of  $T_{c,0}$  are given in Fig. 1(f).

Since *a*-axis lattice constant of the FeTe bulk material is smaller than those of MgO, SrTiO<sub>3</sub>, and LSAT, but larger than that of the LaAlO<sub>3</sub>, the fact shown in Fig. 1(e) that all *c*-axes lattice constants of the films are smaller than that of the FeTe bulk is peculiar. The contradiction to the expectation that the films on LaAlO<sub>3</sub> should be compressed in plane and therefore stretched out of plane suggests that FeTe is quite unique in properties. This may include at least 3 aspects: (1) FeTe intends to expand its lattice in plane regardless of sign of the lattice mismatch, which is possible since epitaxy of thin films is a kind of low dimensional phenomenon providing more freedom for lattice to adjust itself; (2) FeTe can easily shrink its lattice out of plane in case needed; (3) the critical thickness of 90 nm implies smaller elastic modulus, i.e., FeTe being a softer material. The above hypotheses receive strong supports from the recent hydrostatic experimental results on FeTe [15,16] and on FeSe [10,11,19,20], from which the Se-Se bonds between the adjacent FeSe layers are van der Waals force, and FeTe and FeSe are difficult to be compressed in plane, easier to be compressed out of plane, and softer with an elastic modulus as small as only ~30 GPa for FeSe [19].

The FeTe films on different substrates were observed by the SEM, atomic force microscopy, and transmission electron microscopy. The SEM and EDAX results of a FeTe film on SrTiO<sub>3</sub> [Figs. 2(a) and 2(b)] reveal that the film has precipitates of ~150 nm in size on the surface. The EDAX were performed not only on the big area [Fig. 2(b)], but

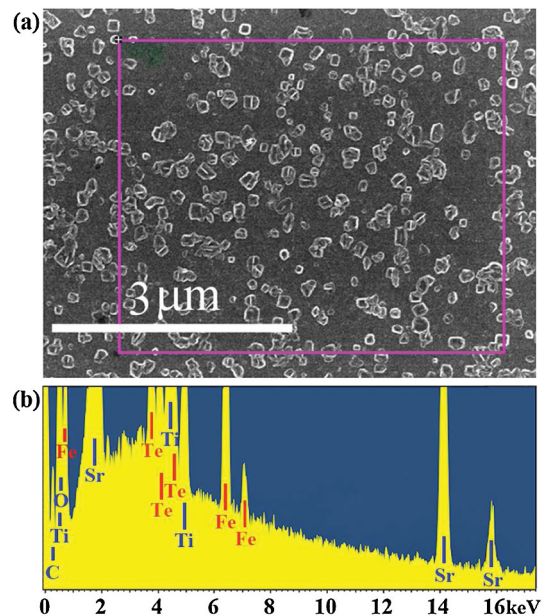


FIG. 2 (color). Scanning electron microscopy and energy dispersive analysis of x-ray. (a) SEM photograph of a FeTe film on SrTiO<sub>3</sub>. (b) EDAX of the surface area within the frame shown in (a), giving a Fe:Te ratio of 1.08:1.

also on the precipitates and on the areas without precipitate. These analyses lead to 2 results: (1) the Fe:Te ratios ranging from 1.04 to 1.10 over 1, (2) no Se contaminations in the FeTe films.

Figure 3 reproduces the temperature dependencies of the resistivity, dc magnetization, and ac susceptibility of a FeTe film on MgO substrate. The starting transition temperature  $T_{c,onset}$  is 13.0 K, and the  $T_{c,0}$  is 9.1 K as shown in Fig. 3(a). Since the magnetization signal is dominated by

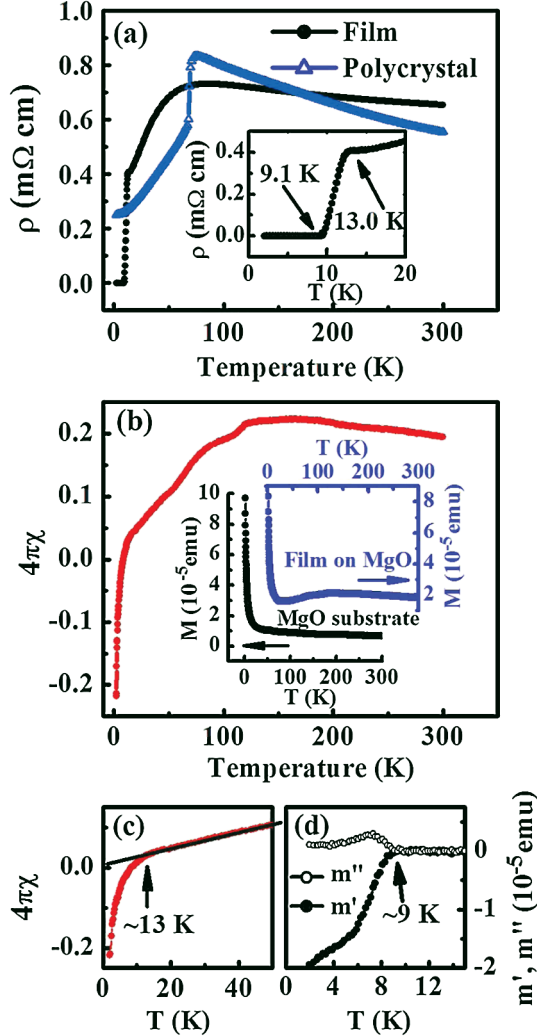


FIG. 3 (color). Resistivity and magnetization versus temperature measurements for a FeTe film on MgO substrate measured from 300 K down to 2 K. (a) Four probe resistivity measurement result for a film and a FeTe bulk crystal given as a reference. Inset gives the enlargement of part of that of the film. The first-order phase transition at 70 K can be seen clearly in the FeTe bulk crystal. (b) Subtraction result of the dc magnetization of the FeTe film, with magnetic field perpendicular to the film surface plane. Inset shows the original dc magnetization measurement results for the FeTe film on MgO, and for the MgO substrate. Measurements were performed under 500 Oe and with the field perpendicular to the film surface. (c) Enlargement of part of the subtraction result in (b). (d) The ac susceptibility measurement result.

the strong paramagnetic contribution from the oxide substrates in low temperature, we subtract the magnetization of the film from that of the film on MgO substrate, as given in Figs. 3(b) and 3(c). The superconducting volume is 22%

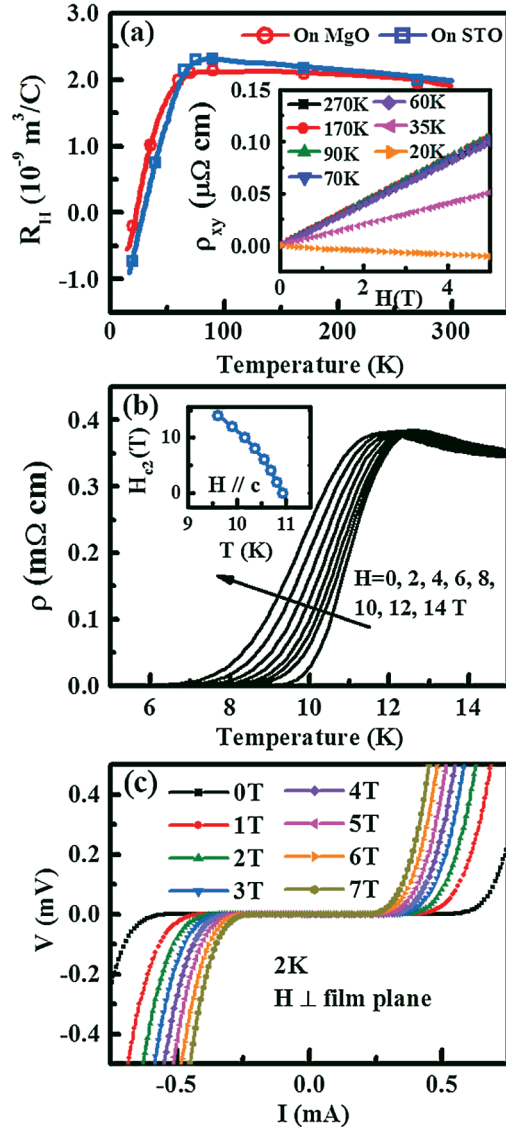


FIG. 4 (color). Transport properties of our FeTe thin films. (a) Temperature dependencies of the Hall coefficients of 90 nm thick FeTe films on MgO and on SrTiO<sub>3</sub> measured at fixed magnetic field 5 T by scanning the temperature. Inset gives the Hall resistivity as a function of applied magnetic field measured at fixed temperatures for the film on MgO. Results from temperature scan and field scan match well to each other. A bar of  $300 \times 900 \mu\text{m}^2$  was etched. (b) Influence of magnetic field on superconductivity for a 90 nm FeTe film on SrTiO<sub>3</sub>. Inset shows upper critical fields deduced from the midpoint transition temperatures with  $H_{c2}(0)$  extrapolated to be 123.0 T. A microbridge of  $10 \times 100 \mu\text{m}^2$  was etched. (c) Current versus voltage measurements for the microbridge given in (b) performed at 2 K under magnetic field up to 7 T. Critical current densities at 2 K under 0 and 7 T are  $6.7 \times 10^4 \text{ A cm}^{-2}$  and  $3.0 \times 10^4 \text{ A cm}^{-2}$ , respectively. Critical currents were read at  $1 \times 10^{-5} \text{ V}$  criteria.

at 2 K, which is much higher than FeSe [3] and close to  $\text{Fe}_{1+\delta}\text{Se}_{0.5}\text{Te}_{0.5}$  [21]. Almost all the film samples show  $T_{c,\text{onset}}$  of 13.0 K, identified by the resistance measurement and the dc magnetization measurement. This value is much higher than that in FeSe bulk [3,22] and thin film [17,22,23] samples. The highest  $T_{c,0}$  observed in resistance measurement is 10.6 K, for a 90 nm thick film on  $\text{SrTiO}_3$ . Further studies should pay attentions to the possible inhomogeneity inside the films which may contribute to the nonbulk superconductivity and relatively large  $\Delta T_c$ .

In nonsuperconducting FeTe bulk samples, a first-order magnetic and structural phase transition occurs at  $\sim 70$  K accompanied by the anomalies in resistivity [Fig. 3(a)], magnetic susceptibility, and Hall coefficient [12–14]. Obviously, this transition is broadened, with maxima or dramatic drop starting at 85.7 K [Fig. 3(a)], 120.2 K [Fig. 3(b)], and 79.3 K/86.2 K [Fig. 4(a)] for the resistivity, susceptibility, and Hall coefficient, respectively. Furthermore, the influences of the magnetic field on superconductivity were investigated [Figs. 4(b) and 4(c)]. The upper critical field  $H_{c2}(0)$  estimated [17] is 123.0 T, much higher than that of FeSe [3,17], and comparable to those of iron pnictides [24]. The current carrying capacities, i.e., the critical current densities  $J_c$  (2 K, 0 T) and  $J_c$  (2 K, 7 T), are  $6.7 \times 10^4 \text{ A cm}^{-2}$  and  $3.0 \times 10^4 \text{ A cm}^{-2}$ , respectively. This suggests that the FeTe films may serve as a good supercurrent carrier under certain magnetic field.

The tetragonal FeTe is in the spotlight because of its theoretical significances: (1) There is increasing consensus that superconductivity in the iron pnictides comes from doping induced suppression of the spin-density-wave (SDW) ground state [25], while whether or not such picture applies fully to the iron chalcogenides is still under debate [26–28]. (2) Density functional study predicted a stronger SDW and therefore a higher  $T_c$  in FeTe than FeSe was expected [29]. Such speculation was growing after 37 K superconductivity was reached under high pressure in FeSe [11] and application of pressure was found to enhance the spin fluctuations [30]. With superconducting FeTe films available, whether or not the SDW exists [26–28] but only being softened as our experiments have indicated will provide testimony to the ongoing debate upon mechanism of iron pnictides and chalcogenides.

In summary, the onset of superconductivity of 13 K has been introduced by interfacial stress, and more specifically by the tensile stress, into the tetragonal nonsuperconducting FeTe compound. We noticed that this can only be realized via stretching the specimen rather than compressing, which can be regarded as a “negative” hydrostatic pressure. FeTe has been regarded as touchstone of several

appealing mechanism proposals. The new findings, the softening of the first-order transition and the increment of bond angles, surely input more ingredients (or say, more constraints) for further theoretical studies on superconducting mechanism.

This work is supported by the MOST of China (2006CB921107 and 2009CB320305) and the NSFC (10774165). L. X. C. and J. L. Y. are also supported by the BRJH of the Chinese Academy of Sciences.

---

\*lxcao@aphy.iphy.ac.cn

- [1] J. P. Locquet *et al.*, Nature (London) **394**, 453 (1998).
- [2] Y. Kamihara, T. Watanabe, M. Hirano, and H. Hosono, J. Am. Chem. Soc. **130**, 3296 (2008).
- [3] F. C. Hsu *et al.*, Proc. Natl. Acad. Sci. U.S.A. **105**, 14262 (2008).
- [4] M. Rotter, M. Tegel, and D. Johrendt, Phys. Rev. Lett. **101**, 107006 (2008).
- [5] J. H. Tapp *et al.*, Phys. Rev. B **78**, 060505(R) (2008).
- [6] X. H. Chen *et al.*, Nature (London) **453**, 761 (2008).
- [7] Z. A. Ren *et al.*, Chin. Phys. Lett. **25**, 2215 (2008).
- [8] H. Takahashi *et al.*, Nature (London) **453**, 376 (2008).
- [9] M. S. Torikachvili, S. L. Bud'ko, N. Ni, and P. C. Canfield, Phys. Rev. Lett. **101**, 057006 (2008).
- [10] Y. Mizuguchi *et al.*, Appl. Phys. Lett. **93**, 152505 (2008).
- [11] S. Medvedev *et al.*, Nature Mater. **8**, 630 (2009).
- [12] S. Li *et al.*, Phys. Rev. B **79**, 054503 (2009).
- [13] W. Bao *et al.*, arXiv:0809.2058v1.
- [14] G. F. Chen *et al.*, Phys. Rev. B **79**, 140509(R) (2009).
- [15] Y. Mizuguchi *et al.*, Physica C (Amsterdam) **469**, 1027 (2009).
- [16] C. Zhang *et al.*, arXiv:0905.3249v2.
- [17] Y. Han *et al.*, J. Phys. Condens. Matter **21**, 235702 (2009).
- [18] L. X. Cao *et al.*, Phys. Rev. B **65**, 113402 (2002).
- [19] J. N. Millican *et al.*, Solid State Commun. **149**, 707 (2009).
- [20] D. Braithwaite *et al.*, J. Phys. Condens. Matter **21**, 232202 (2009).
- [21] B. C. Sales *et al.*, Phys. Rev. B **79**, 094521 (2009).
- [22] M. K. Wu *et al.*, Physica C (Amsterdam) **469**, 340 (2009).
- [23] M. J. Wang *et al.*, Phys. Rev. Lett. **103**, 117002 (2009).
- [24] H. Q. Yuan *et al.*, Nature (London) **457**, 565 (2009).
- [25] M. R. Norman, Physics **1**, 21 (2008).
- [26] A. V. Balatsky and D. Parker, Physics **2**, 59 (2009).
- [27] Y. Xia *et al.*, Phys. Rev. Lett. **103**, 037002 (2009).
- [28] M. J. Han and S. Y. Savrasov, Phys. Rev. Lett. **103**, 067001 (2009).
- [29] A. Subedi, L. Zhang, D. J. Singh, and M. H. Du, Phys. Rev. B **78**, 134514 (2008).
- [30] T. Imai *et al.*, Phys. Rev. Lett. **102**, 177005 (2009).